Diabetes Diminishes Phosphatidic Acid in the Retina: A Putative Mediator for Reduced mTOR Signaling and Increased Neuronal Cell Death

Todd E. Fox,[1,2] *Megan M. Young,*[1] *Michelle M. Pedersen,*[1] *Xianlin Han,*[3] *Thomas W. Gardner,*[*,2,4] *and Mark Kester*[1,2]

Purpose. We demonstrated previously that pro-survival insulin receptor, PI3K-Akt, and p70 S6K signaling is diminished in models of diabetic retinopathy. As mammalian target of rapamycin (mTOR), an upstream activator of p70 S6Kinase is, in part, regulated by lipid-derived second messengers, such as phosphatidic acid (PA), we sought to determine if diminished mTOR/p70 S6Kinase signaling in diabetic retinas may reflect diminished PA levels.

Methods. Alterations in PA mass from retinas of control and streptozotocin-induced diabetic rats were determined by mass spectrometry. The biochemical and biophysical mechanisms underlying the actions of PA on insulin-activated mTOR/p70 S6Kinase signaling were determined using R28 retinal neuronal cells.

Results. We demonstrate a significant decrease in PA in R28 retinal neuronal cells exposed to hyperglycemia as well as in streptozotocin-induced diabetic rat retinas. Exogenous PA augmented insulin–induced protection from interleukin-1β-induced apoptosis. Moreover, exogenous PA and insulin cooperatively activated mTOR survival pathways in R28 neuronal cultures. Exogenous PA colocalized with activated mTOR/p70 S6kinase signaling elements within lipid microdomains. The biochemical consequences of this biophysical mechanism is reflected by differential phosphorylation of tuberin at threonine 1462 and serine 1798, respectively, by PA and insulin, which reduce this suppressor of mTOR/S6Kinase signaling within lipid microdomains.

Conclusions. These results identify PA-enriched microdomains as a putative lipid-based signaling element responsible for mTOR-dependent retinal neuronal survival. Moreover, diabetic retinal neuronal apoptosis may reflect diminished PA mass. Elevating PA concentrations and restoring mTOR signaling may be an effective therapeutic modality to reduce neuronal cell death in diabetic retinopathy. (*Invest Ophthalmol Vis Sci.* 2012;53:7257–7267) DOI:10.1167/iovs.11-7626

Retinal degeneration due to neuronal cell death is an underlying cause of many visual diseases, including retinitis pigmentosa, macular degeneration, and diabetic retinopathy. We and others have shown that there is an increased rate of neuronal apoptosis in diabetic animal models and in retinas of patients with diabetes.[1–4] Therefore, understanding the regulation of pro-survival signaling cascades may identify therapeutic targets to treat such retinal neurodegenerative diseases.

One potential regulator of survival is mammalian target of rapamycin (mTOR), a pro-translational/pro-mitogenic/pro-survival effector, which is altered in multiple diseases, including cancer, atherosclerosis, and diabetes.[5] mTOR is well known to mediate amino acid- and growth factor-induced translation, and there is increasing evidence for the role of mTOR and its downstream effectors in the regulation of cellular survival.[6] In fact, p70 S6Kinase (S6K) also is implicated in regulating cell survival by inactivating the pro-apoptotic protein BAD via phosphorylation at Ser^{136}.[7] It has been demonstrated that mTOR-dependent regulation of protein phosphatase-2A[8] and protein phosphatase-5[9] are important for cell survival. Furthermore, mTOR signaling regulates autophagy in mammalian cells.[10] We showed recently that p70 S6K, a downstream effector of mTOR, is an important factor in mediating insulin-induced survival of retinal neurons.[11] Taken together, dysfunctional mTOR/p70S6Kinase activity can contribute to retinal neuron death in models of diabetes.

Of potential clinical importance, we demonstrated that Akt and p70 S6K signaling, which are regulated by the mTOR complexes mTORC2 and mTORC1, respectively, are suppressed in the diabetic rat retina.[12] Therefore, as mTOR complexes are upstream of Akt and p70 S6K, understanding the mechanisms by which mTOR signaling is regulated could have therapeutic implications for inhibiting retinal neurodegeneration. One putative neurodegenerative factor is interleukin-1β (IL-1β), which is increased in the diabetic retina,[13–15] and has an important role in mediating neurodegeneration caused by ischemic and excitotoxic conditions in the retina

From the Departments of [1]Pharmacology, [2]Cellular and Molecular Physiology, and [4]Ophthalmology, Penn State College of Medicine, Hershey, Pennsylvania; and the [3]Division of Bioorganic Chemistry and Molecular Pharmacology, Department of Medicine, Washington University School of Medicine, St. Louis, Missouri.

Supported in part by grants with the Pennsylvania Department of Health using Tobacco Settlement Funds (to MK and Core Facility services and instruments [ABI 4000 QTrap] used in this project), and by the Juvenile Diabetes Research Foundation Diabetic Retinopathy Center (#4-2002-455, project 3 to MK), a JDRF postdoctoral fellowship (to TEF), the American Diabetes Association (to MK), and EY018336 (to MK and TEF) and EY020582 (TWG) from the National Eye Institute. TWG is the Jack and Nancy Turner Professor. MK is the G. Thomas Passananti Professor. The authors alone are responsible for the content and writing of the paper.

Submitted for publication March 31, 2011; revised March 25 and August 8, 2012; accepted August 13, 2012.

Disclosure: **T.E. Fox**, None; **M.M. Young**, None; **M.M. Pedersen**, None; **X. Han**, None; **T.W. Gardner**, None; **M. Kester**, None

Current affiliation: *The Kellogg Eye Center, University of Michigan Medical School, Ann Arbor, Michigan.

Corresponding author: Mark Kester, Department of Pharmacology R130, Penn State College of Medicine, Hershey, PA 17033; mkester@psu.edu.

and brain.[16–18] In fact, cerebral ischemia suppresses protein synthesis and p70 S6K phosphorylation.[19] Thus, understanding the mechanisms responsible for cell stress-induced mTOR/p70S6 kinase-induced retinal cell death may identify new targets for treatments of diabetic retinopathy.

Hypoxic stress, ischemia, inflammatory cytokines, and diabetes all stimulate phospholipid catabolism and generation of lipid-derived second messengers, yet the roles of these lipid-derived second messengers with regard to mTOR/p70 S6K activity in stress-induced states have not been investigated in retinal neurons to our knowledge. In particular, phosphatidic acid (PA), which typically is generated through the phosphorylation of diglycerides by diglyceride kinases or the activation of phospholipase D (PLD), has been demonstrated to regulate positively mTOR signaling.[20–22]

The regulation of mTOR signaling by PA could be direct (biochemical) and/or indirect (biophysical). The biophysical regulation, organization, and coordination of signaling cascades is controlled within lipid rafts, also called lipid microdomains, which include caveolae. It is thought that lipid rafts serve as signalosome assembly platforms to coordinate the interactions between scaffold and anchoring proteins with kinases for efficient downstream signaling.[23,24] It is hypothesized specifically that PA within cholesterol-enriched lipid microdomains can augment mTOR signaling, and that an underlying cause of diminished mTOR/p70 S6Kinase signaling in diabetic retinas may reflect diminished PA concentration. Elevating PA concentrations and restoring mTOR signaling may be an effective therapeutic modality to reduce inflammatory cytokine-induced neuronal cell death in diabetic retinopathy.

Materials and Methods

Materials

Bovine insulin and nystatin were purchased from Sigma (St. Louis, MO). Laminin and cell permeable cAMP were from BD Biosciences (Franklin Lakes, NJ) and MP Biomedicals (Irvine, CA), respectively. PA and nitrobenzoxadiazole (NBD)-PA was purchased from Avanti Polar Lipids (Alabaster, AL). ^{14}C-labeled PA was purchased from American Radiolabeled Chemicals, Inc. (St. Louis, MO). Polyclonal rabbit anti-phospho-p42/44 MAPK (Thr^{202}/Tyr^{204}), rabbit anti-p42/44 MAPK, anti-phospho-p70 S6K Thr^{389}, anti-p70 S6K, anti-p90 RSK Ser^{380}, anti-RXRXXpS/T, anti-tuberin phospho-Thr^{1462}, GAPDH, and β-actin antibodies were obtained from Cell Signaling Technology (Beverly, MA). Anti-rabbit IgG-horseradish peroxidase, anti-tuberin, anti-ERK2, and insulin receptor β antibodies were obtained from Santa Cruz Biotechnology (Santa Cruz, CA). siRNA to PLD1 (s128963) was obtained from Applied Biosystems (Carlsbad, CA).

Cell Culture

R28 cells, a rat retinal cell line, were a generous gift from Gail M. Seigel, State University of New York, Buffalo.[25] They were grown in Dulbecco's modified Eagle's medium (DMEM) containing 5.5 mM glucose supplemented with 10% newborn calf serum (Hyclone, Logan, UT). The cells were differentiated to neurons on laminin-coated plates or coverslips with addition of 25 μM cell-permeable cAMP as described previously.[26]

Animals

Male Sprague-Dawley rats, approximately 200 g (Charles River Laboratories, Wilmington, MA), were fasted overnight and given a single intraperitoneal injection of streptozotocin (STZ, 65 mg/kg; Sigma), freshly dissolved in 10 mM sodium citrate buffer (pH 4.5). Diabetes was confirmed 6 days later by blood glucose greater than 250 mg/dL (Lifescan, Milpitas, CA). Age-matched control and diabetic rats were monitored regularly by weight and blood glucose tests. Rats were housed in accordance with the Institutional Animal Care and Use Committee guidelines, and the study protocol adhered to the ARVO Statement for the Use Animals in Ophthalmic and Vision Research. Rats were maintained by the Juvenile Diabetes Research Foundation Animal Core Facility at Penn State University and group housed in solid plastic bottom cages with bedding as well as ad libitum food (Teklad Global 18% Protein Rodent Diet; Harlan Laboratories, Indianapolis, IN) and water under a normal 12-hour light-dark schedule. Retinas were dissected after 4 weeks of diabetes and snap frozen in liquid N_2. The average weight on the day of sacrifice was 375.3 ± 6.5 g for controls versus 234.8 ± 8.3 g for the STZ-induced diabetes. The blood glucose of the animals was 109.5 ± 2.5 mg/dL for controls versus 509.6 ± 28.9 mg/dL for the STZ-induced diabetic rats. There were 8 animals in each group.

Mass Spectrometry

Lipids were extracted from retinas using a modified acidified Bligh and Dyer extraction protocol after addition of a 14:0-14:0-PA internal standard. Lipid extracts were analyzed on a LTQ-Orbitrap mass spectrometer or an ABI 4000 QTrap, essentially as described previously.[27]

PA Determination by TLC

TLC was used also to assess PA levels. R28 cells were treated as described in the text and ^{32}P-orthophosphate.was added at 20 μCi/mL for the last 4 hours of culture before subjecting cells to lipid extraction by a Bligh and Dyer extraction protocol. Labeled PA was detected by TLC separation using chloroform/methanol/acetone/acetic acid/water (50:10:20:10:5) as the developing solvent. PA was detected using authentic standards obtained from Avanti Polar Lipids (Alabaster, AL) and the PA bands were scraped off and the radioactivity measured by scintillation counting.

Western Blot Analysis

Western blot analyses were performed essentially as described previously.[26] Briefly, treated R28 cells were washed in ice-cold Dulbecco's phosphate-buffered saline solution and lysis buffer (50 mM HEPES, 137 mM NaCl, 5 mM NaF, 1 mM EDTA, 1 mM EGTA, 1 mM Na_3VO_4, 1% NP-40, Protease Inhibitor Cocktail [Roche Applied Science, Indianapolis, IN]) was added. Cell lysates were cleared by centrifugation, and the Bio-Rad DC protein assay was used to determine protein concentration. Typically 30 μg of protein lysate per sample were separated on 4–12% NuPAGE gels (Invitrogen, Carlsbad, CA) and transferred to Hybond nitrocellulose membranes (GE Healthcare, Piscataway, NJ). The membranes subsequently were immunoblotted and visualized by ECL (GE Healthcare). Bands were quantified using ImageQuant (Molecular Dynamics, Sunnyvale, CA), or GeneTools SynGene (K&R Technology, Frederick, MD) software. For immunoprecipitation, 2 μg of anti-tuberin or anti-insulin receptor μ antibody were incubated with 400 or 200 μg, respectively, of protein lysate overnight. The next day, protein G was added for 1 hour, and the complex subsequently was washed twice with lysis buffer and analyzed by Western blotting.

Cellular Fractionation

For the PA localization study, R28 cells were treated as described in the text and a detergent-free method of isolating lipid rafts was performed as described previously.[28] Briefly, cells were harvested in sodium carbonate buffer (pH 11.0) and homogenized. Homogenates were adjusted to 4 mL with 90% sucrose in MES-buffered saline (MBS) (25 mM MES, pH 4.5, 150 mM NaCl, 1 mM sodium orthovanadate, 1 mM NaF, protease inhibitor tablet) to a final concentration of 45% sucrose. Samples were layered at the bottom of a 14 × 89 mm tube containing 4

mL each of 35% and 5% sucrose in sodium carbonate/MBS and centrifuged in a Beckman SW41ti rotor at 200,000*g* for 16 to 20 hours at 4°C. Serial fractions of 1 mL were removed and analyzed subsequently by dispensing 200 μL of each fraction to a microtiter plate in triplicate and the fluorescence was measured with a Molecular Devices SpectraMax Gemini XS plate reader.

For protein localization to Triton X-100-insoluble fractions, an adapted methodology was used.[29] Briefly, R28 cells were homogenized in a buffer containing 10 mM HEPES pH 7.4, 1 mM EDTA, 250 mM sucrose, 5 mM NaF, 1 mM β-glycerolphosphate, 1 mM Na_3VO_4, and protease inhibitors, and passed through a 22-gauge needle several times. After centrifugation at 10,000*g* for 10 minutes to remove unbroken cells and nuclei, this supernatant was spun at 100,000*g* for 45 minutes to isolate cytosolic and microsomal fractions. The microsomal pellet was resuspended in a 1% Triton X-100 buffer and incubated on ice for 30 minutes before being spun at 100,000*g* again. The resulting pellet was resuspended in 1% SDS and 20 βg of protein from each fraction (cytosolic, Triton X-100 soluble, Triton X-100 insoluble/SDS soluble) then were analyzed by Western blotting.

Cell Death Quantification

R28 cells were cultured on glass coverslips and treated as described in the text. After treatment, cells were washed in PBS and fixed in 2% paraformaldehyde before staining/mounting with Vectashield mounting medium with DAPI (Vector Laboratories, Burlingame, CA). Five randomly sampled fields from each coverslip were observed to determine the percent of pyknotic nuclei as described previously.[26]

Cholesterol Measurement

Cholesterol was measured using a Cholesterol Assay Kit from Cayman Chemical (Ann Arbor, MI) following the manufacturer's instructions. Cholesterol esterase was excluded from the protocol, so only non-esterified, "free" cholesterol was measured.

mTOR Kinase Activity Assay

TOR activity was assessed by immunoprecipitation of TOR from 500 μg of R28 cell lysate with a mTOR specific antibody (a custom rabbit polyclonal antibody provided generously by Scot Kimball, Penn State University) and protein A agarose. Washed immunoprecipitates subsequently were incubated with recombinant PHAS-1 (4EBP1) (Santa Cruz Biotechnology) and ^{32}P-ATP (American Radiolabeled Chemicals, St. Louis, MO) in 50 mM NaCl, 10 mM HEPES (pH 7.5), 10 mM $MnCl_2$, 50 mM β-glycerophosphate, 1 mM DTT, and 1 mM sodium orthovanadate, and incubated for 10 minutes at 30°C. The reaction then was separated by SDS-PAGE, transferred to nitrocellulose, and exposed to film to detect radiolabeled 4EBP1 protein.

RNA Isolation and Quantitative RT-PCR

Total RNA was isolated using the RNEasy purification system (Qiagen, Valencia, CA). Quality and quantity were assessed using the RNA 6000 Nano LabChip with a 2100 Expert Bioanalyzer (Agilent, Palo Alto, CA). Quantitative PCR analysis was performed using the 7900HT Sequence Detection System. The $2^{-\Delta\Delta Ct}$ analysis method was used to quantify relative amounts of mRNAs using β-actin as an endogenous control. The gene expression assay used to detect the phospholipase D1 gene (*pld1*) was Rn01493709 (Applied Biosystems).

Statistical Methods

One-way ANOVA with Bonferroni multiple comparison post test and *t*-tests analysis were performed using GraphPad Prism 4.0 software, with statistical significance considered if $P < 0.05$. All data shown are from a minimum of $n = 3$ separate biologic experiments.

Results

PA Content Is Diminished in Models of Diabetic Retinopathy

We, and others, previously observed altered fatty acids, neutral lipid, phospholipid, and sphingolipid metabolism in models of diabetic complications, including diabetic retinopathy.[30,31] Therefore, we focused on measuring PA, a phospholipid that has been implicated in regulation of mTOR/p70 S6Kinase prosurvival/promitiogenic signaling. First, we tested if hyperglycemic insults alter PA mass in R28 cells, a rat-derived model of retinal neurons.[26] Here, R28 cells were grown for 72 hours under basal media (5.5 mM glucose), 25 mM glucose, or mannitol (5.5 mM glucose plus 19.5 mM mannitol) as an osmotic control. In the last 4 hours, ^{32}P-orthophosphate was added to label cellular phospholipids. After examining PA content via TLC, we observed that 25 mM glucose, but not equimolar mannitol, significantly reduced the production of PA (Fig. 1A). Thus, a hyperglycemic environment leads to reductions in PA content.

We next tested if a similar process occurs in vivo in STZ-induced diabetic rats (4 weeks duration), a model of type 1 diabetes. At this time point, the rate of cellular apoptosis has reached the maximum and sustained rate.[2] Retinal lipid extracts were assessed from these animals and aged-matched controls for PA levels by mass spectrometry. Overall, we observed a 23.4% decrease in PA levels ($P = 0.014$, Fig. 1B). Specifically, this decrease is attributed predominately to 16:0-18:1-PA and PA-species containing docosahexanoic acid (22:6) fatty acids (Fig. 1C). These data demonstrate that diabetes-induced hyperglycemia rapidly reduces PA levels in the retina, concomitant with accelerated cell death.[2]

Insulin and PA Rescue R28 Cells from IL-1β–Induced Death

Insulin treatment limits neuronal cell death in rodent models of diabetic retinopathy.[2] Furthermore, inhibition of diacylglycerol kinase, an enzyme that generates PA at the expense of diacylglycerol (DAG), mimics diabetes-induced abnormal retinal hemodynamics.[32] Thus, altering DAG or phospholipid metabolism to form PA may be therapeutically desirable. To test this hypothesis initially, we used exogenous PA as a therapeutic modality to support retinal neuronal survival under conditions of diabetic stress. We reported previously that hyperglycemia per se does not induce cell death of R28 cells, but rather inhibits pro-survival signaling.[33] This is not surprising as primary retinal cells only demonstrate a small decrease in viability (~8%) in a hyperglycemic environment with prolonged treatment.[34] The pro-inflammatory cytokine IL-1β is upregulated in the diabetic rat retina,[13–15] and is elevated in the vitreous and sera of patients with diabetes,[35] and IL-1β can be a mediator of neurodegeneration.[16–18] We, therefore, determined if the ability of insulin and/or PA to regulate pro-survival pathways positively could prevent IL-1β-induced cellular death. When R28 cells were treated with IL-1β (10 ng/mL, based on previous work[36]) 26% of the remaining attached cells were pyknotic (Fig. 2A). PA reduced this apoptosis significantly by half to 13%, whereas insulin reduced apoptosis significantly to 18% in the presence of IL-1β. When R28 cells were treated with PA and insulin in the presence of IL-1β, apoptosis was reduced further toward the control value (8%), which was significantly less compared to PA or insulin alone in the presence of IL-1β. However, in the presence of rapamycin, an inhibitor of mTOR, the ability of PA, insulin, and both insulin and PA together to inhibit IL-1β-induced cellular death was diminished significantly. While rapamycin did not

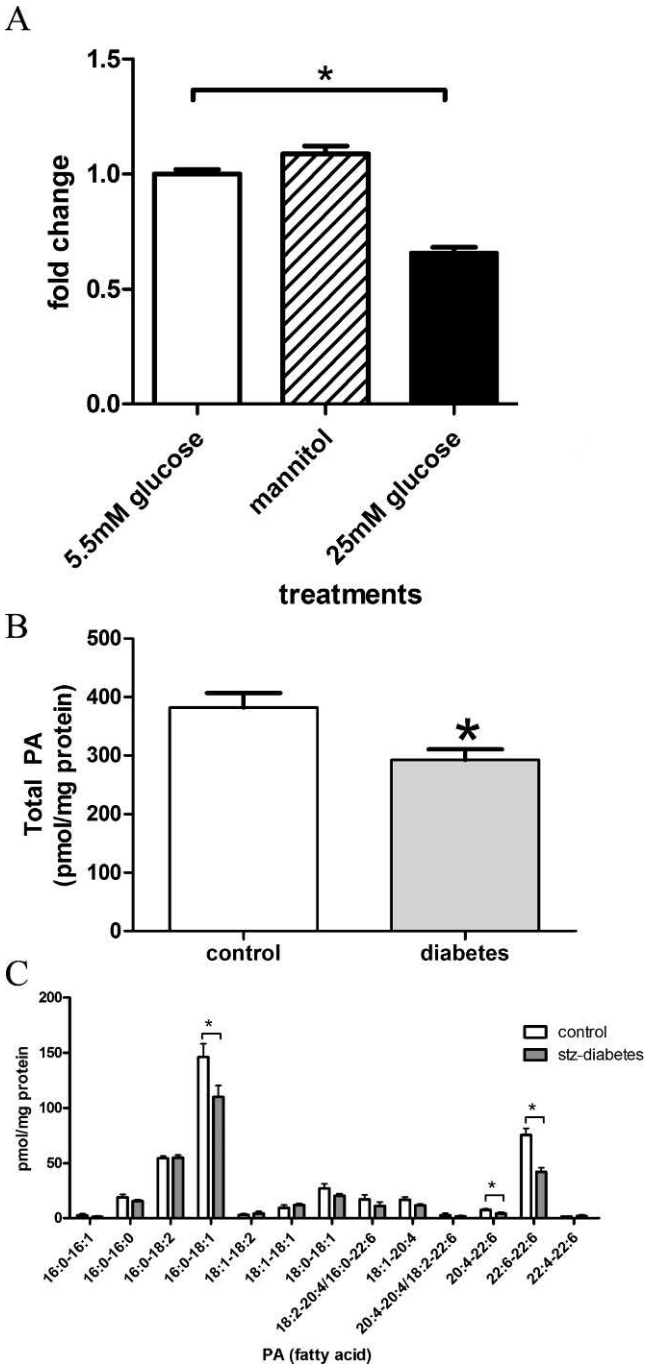

Figure 1. Hyperglycemia and diabetes reduce PA levels in retina models. (**A**) R28 cells were grown under the indicated conditions for a total of 72 hours and labeled with ^{32}P-orthophosphate. PA was detected after TLC separation ($n = 4$ independent experiments for each treatment). The overall P value upon analysis by one-way ANOVA was <0.0001, $F = 76.25$. Bonferroni post-hoc comparison reveals that 5.5 mM and mannitol (5.5 mM glucose + 19.5 mM mannitol) groups are significantly different than 25 mM glucose treatment, but are not significant from each other. (**B**) Retinal lipid extracts from 4-week STZ-induced diabetic rats and age-matched controls ($n = 8$ rats per group) were assessed for PA by mass spectrometry. We observed that total PA levels were reduced significantly in diabetes. (**C**) When comparing the fatty acid chains of PA, we noted significant reductions in 22:6 (DHA) containing PA and a reduction of 16:0-18:1 PA. $^* = P < 0.05$. All *error bars* represent SE.

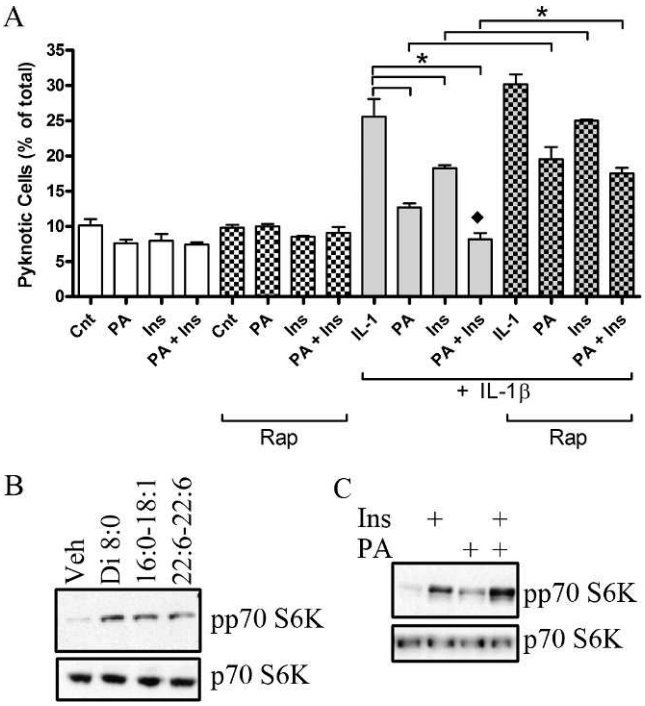

Figure 2. PA and insulin cooperatively rescue retinal neurons from IL-1β–induced apoptosis. (**A**) R28 cells were treated with vehicle, insulin (10 nM), PA (50 μM), or insulin and PA in the presence or absence of IL-1β (10 ng/mL) and/or rapamycin (100 nM) for 24 hours. The number of pyknotic nuclei was determined by DAPI staining, then counted and expressed as a percentage of the total number of cells. ($P < 0.0001$ ANOVA $F = 54.53$, $^*P < 0.05$; $n = 3$ independent experiments per condition, ◆ significantly different from PA + IL-1β and Ins + IL-1β). (**B**) R28 cells were serum-starved for 4 hours before stimulation with PAs of different fatty acid compositions for 15 minutes. Western blots then were performed to assess p70 S6K Thr^{389} phosphorylation and p70 S6K (~70 kilodaltons [kDa] molecular weight) levels. A representative blot from $n = 3$ independent biologic experiments is shown. (**C**) R28 cells were stimulated with either insulin (10 nM), PA (50 μM), or insulin and PA simultaneously for 15 minutes, before Western blotting was performed to assess the levels of phosphorylated and total p70 S6K. A representative blot from at least $n = 3$ independent biologic experiments per condition is shown.

block the survival effects of insulin or PA completely, it does imply that a rapamycin-sensitive mTOR signaling may be, in part, an important cascade to limit IL-1β–induced cellular death. This finding also implies that lipid-derived mediators, such as PA, could serve as therapeutic agents to promote survival of retinal neurons under inflammatory conditions in which the normal pro-survival pathways are impaired.

To support further the finding that exogenous PA could protect against stress-induced neuronal death, we assessed the effects of PA directly on p70 S6 kinase activity. When R28 cells were stimulated with various PA species (15 minutes), PA containing two 8-carbon length fatty acid chains (diC8), a palmitate and oleate chain (16:0-18:1) or two docosahexaenoic acid fatty acids (22:6-22:6), we observed a robust increase in p70 S6K phosphorylation at Thr^{389} (Fig. 2B). These results demonstrated that exogenous addition of PA leads to activation of pro-survival p70 S6K, which does not appear dependent on PA fatty acid composition.

As we observed a cooperative effect between insulin and PA on survival (Fig. 2A), we next determined if insulin and PA would cooperatively activate p70 S6K (Fig. 2C). As expected, insulin and PA independently activated p70 S6K. When both were used simultaneously, we observed a 29.5% increase ($P <$

0.01) in p70 S6K phosphorylation compared to insulin alone. Taken together, insulin and PA cooperatively activated p70 S6 kinase.

PA and Insulin Differentially Stimulate mTOR Signaling

We reported previously that p70 S6K activity is diminished in the diabetic rat retina and regulates insulin-induced retinal neuronal cell survival in vitro.[11,12] Studies by others have demonstrated that PA can regulate mTOR signaling, including p70 S6K[22,37] and our data (Fig. 2) support a role for PA in regulating mTOR/p70 S6 kinase-dependent cell survival. To determine if there is overlap between insulin and PA signaling to mTOR, we investigated if insulin activated mTOR through PA generation. We first inhibited phospholipase D, which produces PA predominantly from phosphatidylcholine, by pretreatment with 1-butanol (Fig. 3A). Butanol inhibits putative PA generation and subsequent PA-induced signaling through a transphosphatidylation reaction, which forms phosphatidylbutanol (Ptdbutanol) at the expense of PA. Figure 3A demonstrates that phosphorylation of p70 S6K in response to insulin was unaffected by the presence of 1-butanol ($P = 0.76$). In contrast, as a positive control, phorbol ester (PMA)-induced activation of p70 S6K, but not ERK, was blocked completely in the presences of 1-butanol. To confirm that 1-butanol treatment lowered PMA-induced PA concentration, we assessed PA and Ptdbutanol levels through a similar TLC-based ^{32}P-orthophosphate incorporation ^{32}P-orthophosphate incorporation methodology, as described for Figure 1A. We observed a reduction in PMA-induced, but not basal, PA levels with 1-butanol, with a concomitant increase in Ptdbutanol levels (data not shown). We next validated these 1-butanol-based studies through the use of RNA interference. Small interfering RNA (siRNA) to PLD1 diminished *pld1* mRNA levels by 65% ($P < 0.01$) as assessed by real-time RT-PCR (Fig. 3B). Confirming the butanol data in Figure 3A, PLD1 knockdown did not alter insulin-induced activation of p70 S6K (Fig. 3C, $P = 0.81$). As there are multiple non-PLD-based pathways that can produce PA, we next assessed if insulin could elevate PA levels in R28 cells by mass spectrometry (Fig. 3D). Here, we demonstrated that after 15 minutes of insulin treatment, no overall significant changes were observed in PA content ($P = 0.74$), and no changes in specific species (different fatty acyl groups) were observed (data not shown). Taken together, these results demonstrated that insulin does not induce directly PA generation, and that insulin and PA activate mTOR/p70 S6K through distinct pathways.

TOR Signaling Molecules Localize to Triton X-100 Insoluble Membrane Microdomains

We next asked if the cooperative, but independent, actions of insulin and PA on mTOR signaling elements could be explained through a biophysical mechanism. Lipid microdomains associate dynamically to form platforms for membrane protein sorting and construction of signaling complexes to allow for efficient downstream signaling in response to many ligands.[23] The role of microdomains to regulate cooperatively insulin-stimulated mTOR signaling is defined poorly. Thus we first determined if mTOR signaling components are localized within cholesterol-enriched lipid microdomains. We explored the detergent resistance, a characteristic of lipid microdomains, of several TOR signaling elements in response to PA treatment through ultracentrifugation and solubilization of the resultant membranes, first in Triton-X and then SDS. In Figure 4A, we find that even though mTOR distributes to all three fractions obtained by this procedure, the majority of p70 S6K exists in

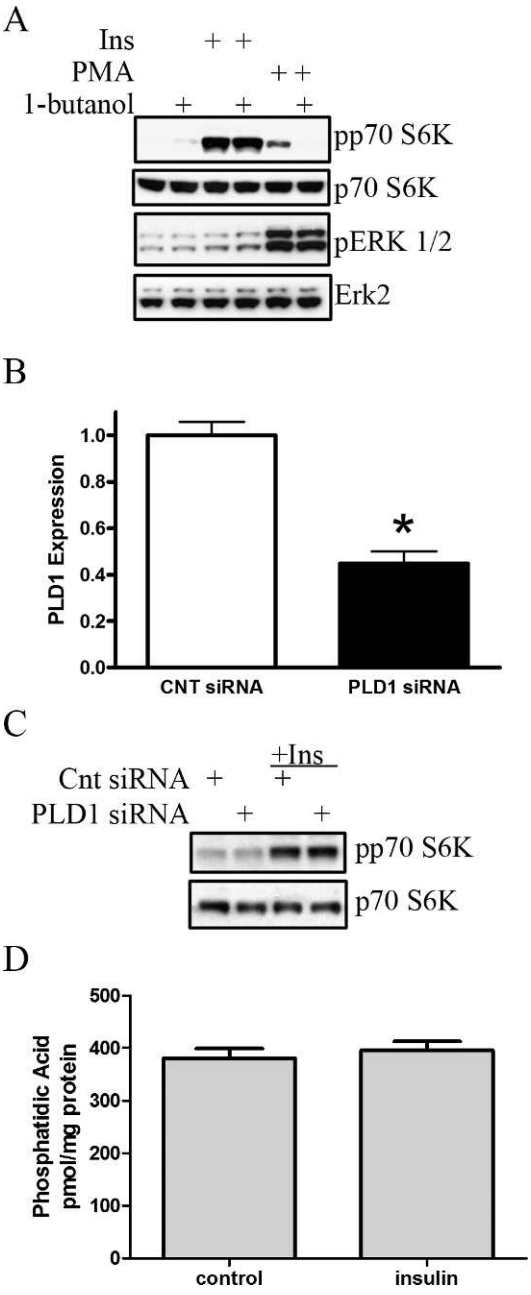

Figure 3. Insulin does not increase endogenous PA production to activate mTOR signaling. (**A**) R28 cells were pretreated with 1-butanol (0.3%, 15 minutes) before stimulation with insulin (10 nM, 15 minutes) or PMA (100 nM, 15 minutes). Western blots were performed to assess the phosphorylation state of p70 S6K and Erk 1/2 (44 and 42 kDa, respectively). Blots are representative of at least three independently performed experiments. (**B**) RNA interference was used to diminish PLD1 expression. Here, knockdown is confirmed by qRT-PCR after transfection with a control scrambled siRNA or siRNA to PLD1. (**C**) R28 cells, transfected with either scrambled or PLD1 siRNA subsequently were stimulated with insulin (10 nM, 15 minutes). Western blots were performed to assess levels of phosphorylated and total p70 S6K. Blots are representative of $n = 3$ independent biologic experiments. (**D**) Serum-starved R28 cells were stimulated with 10 nM insulin for 15 minutes, and the lipids were extracted and assessed for PA content by mass spectroscopy ($n = 4$ independent biologic experiments per group). All *error bars* represent SE. $^*P < 0.05$.

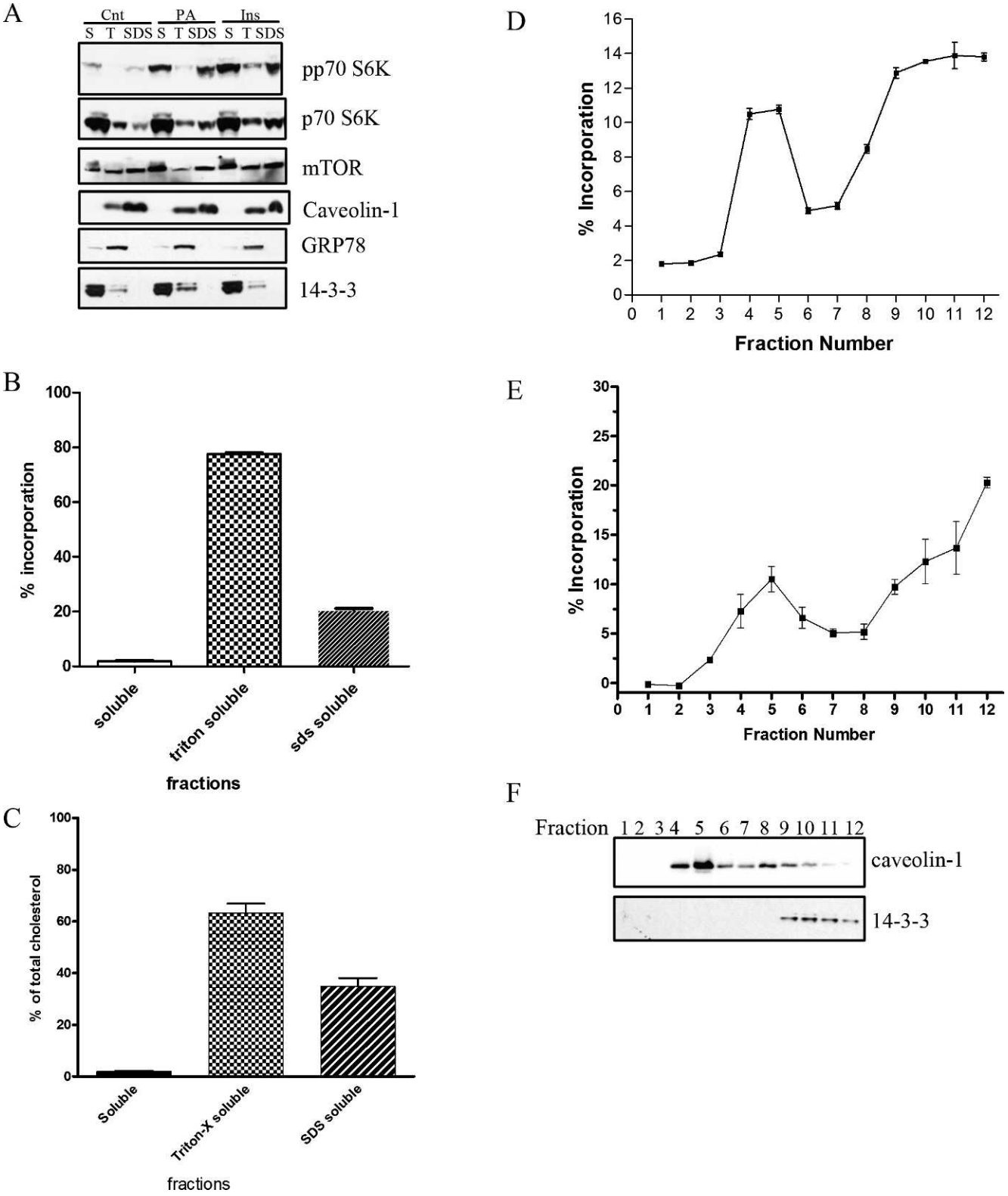

Figure 4. PA- and insulin-induced mTOR signaling is regulated within lipid microdomains. (**A**) Treated R28 cells were fractionated at 100,000*g*, to which the pellet was extracted with 1% Triton-X and spun again at 100,000*g*. The resultant pellet was resuspended in 1% SDS. The fractions, cytosolic/soluble (S), TritonX-100 soluble (T), and SDS solubilized (SDS) were analyzed by Western blotting for various mTOR signaling elements (p70 S6K and mTOR), and fractionation control proteins (caveolin-1 [24 kDa], GRP78 [78 kDa], and 14-3-3 [28 kDa]). Blots are representative of four independent biologic experiments. Similarly, these fractions were analyzed after treatment with NBD-labeled PA (**B**) and for cholesterol content (**C**, data obtained from $n = 3$ independent biologic experiments). Similarly, low buoyant fractions were isolated from R28 cells in a sodium carbonate sucrose gradient after treatment with an NBD-labeled PA (**D**) or ^{14}C-labeled PA (**E**, data obtained from $n = 4$ independent biologic experiments). Successful fractionation was assessed by performing Western blots for caveolin-1 and 14-3-3 on the sucrose gradient fractions (**F**, representative blot of at least four independent experiments).

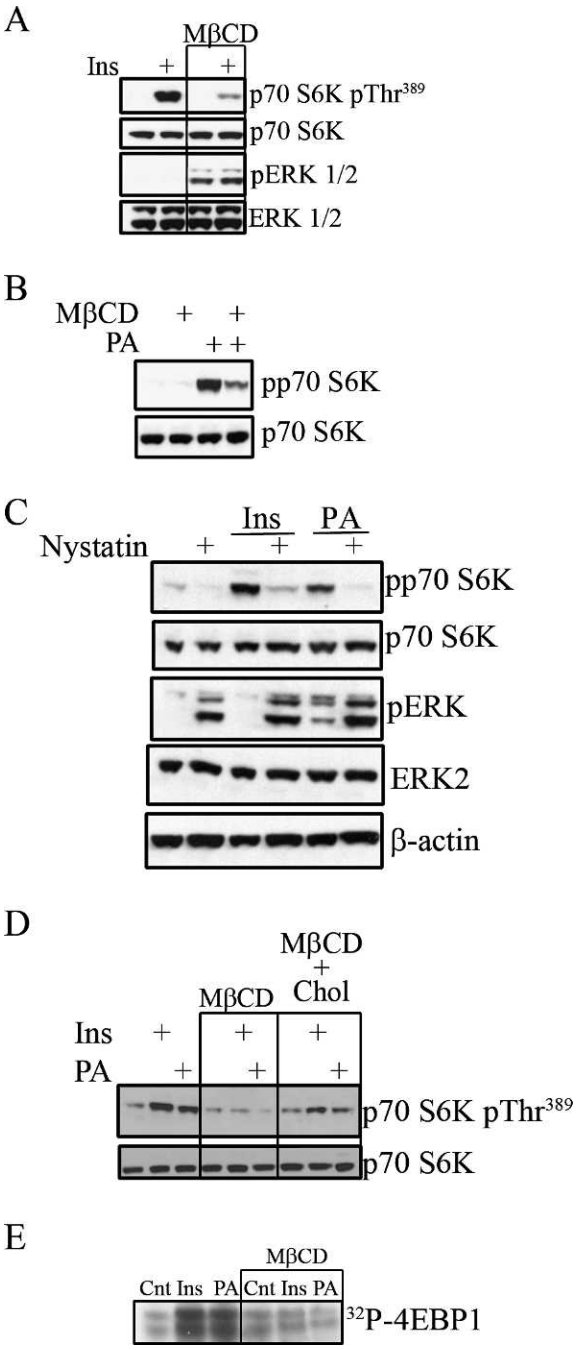

Figure 5. Cholesterol depletion disrupts PA- and insulin-induced TOR signaling. (**A**) R28 cells were pretreated with MβCD (1%, 1 hour) and subsequently treated with insulin (10 nM, 15 minutes). Western blots were used to assess the phosphorylation state of p70 S6K and Erk 1/2. (**B**) The phosphorylation state of p70 S6K also was assessed after cholesterol depletion (MβCD: 1%, 1 hour) before PA treatment (50 μM, 15 minutes). Blots are representative of at least 3 independently performed experiments. (**C**) In a similar manner, R28 cells were pretreated with nystatin (50 μg/mL, 30 minutes) and treated subsequently with insulin or PA. A representative Western blot from a single $n = 3$ experiment is shown demonstrating the phosphorylation state of p70 S6K and Erk 1/2. (**D**) R28 cells were pretreated again with MβCD and treated subsequently with insulin or PA with or without repleting cells with cholesterol (100 μM, 30 minutes). Western blots were used to assess p70 levels and the phosphorylation state of p70 S6K. Representative blots from at least three independently performed experiments are shown. (**E**) A reconstitution kinase assay on immunoprecipated mTOR was performed by assessing the ability to transfer radiolabeled ATP to recombinant 4EBP1 after insulin or PA treatment in the presence of absence of MβCD. Representative radiograph of $n = 3$ separate experiments.

the soluble, non-microsomal fraction (S). Upon examining the phosphorylation of p70 S6K at Thr^{389}, we observed that this phosphorylated form localizes predominantly to the (S) fraction as well as the SDS-solubilized (Triton X-100 insoluble) SDS fractions. The total amount of p70 S6K is less in the SDS fraction (22.8 ± 5.4% SE), as compared to the S fraction (48.3 ± 3.9% SE, $P = 0.019$). In addition, these results demonstrated that a greater percentage of phosphorylated/active to total p70 S6K localizes to the Triton X-100 detergent insoluble (SDS) fraction (52.7 ± 5.9% SE) compared to the (S) fraction (32.2 ± 2.4% SE, $P < 0.05$) or T fraction (15.2 ± 3.5% SE, $P < 0.01$). The lipid microdomain marker, caveolin-1, localized exclusively to the Triton X-100 soluble (T) and insoluble (SDS) fractions in R28 retinal neuronal cells, while GRP78, a protein localized within the endoplasmic reticulum, was localized almost completely to the Triton-x soluble fraction (T) and not the (SDS) fraction. Taken together, these results demonstrated that components of the activated mTOR/p70 S6 kinase signaling cascade are localized to a fraction consistent with lipid microdomains.

We next explored if PA also localizes to fractions consistent with lipid microdomains. First, we treated R28 cells with a fluorescently-labeled NBD-PA. Here, we observed 20% localization to the triton-x insoluble (SDS) fraction (Fig. 4B). To validate this methodology further, we also measured cholesterol content from these fractions and found that 36.7% of the cholesterol also existed in this fraction (Fig. 4C), which is consistent with the results of others,[38] who followed ^{3}H-cholesterol within triton-soluble and triton-insoluble fractions from fibroblasts. Secondly, we isolated low buoyant fractions by detergent-independent sucrose gradient methodologies, and consistent with Figure 4B, when R28 cells were treated with a fluorescently labeled NBD-PA, 22% of exogenously added PA localized to fractions 4 and 5 of a discontinuous sucrose gradient (Fig. 4D). To rule out that the fluorescent NBD label affects PA distribution, we also used a ^{14}C-labled PA (Fig. 4E). Here, we again observed 20% localization to the buoyant fractions, demonstrating that the NBD label does not alter the localization of PA. These fractions (4 and 5) are consistent with lipid-microdomain-enriched fractions, as evidenced by strong localization of the lipid raft marker caveolin-1, but not 14-3-3, to these fractions (Fig. 4F). Taken together, we demonstrated that elements of the insulin-stimulated mTOR signaling cascade co-localize within a PA-enriched lipid microdomain.

Activation of p70 S6K, but Not ERK, Depends on Cholesterol-Enriched Lipid Microdomains

As elements of mTOR signaling reside within functional lipid microdomains, we examined the consequence of lipid raft disruption at the level of p70 S6K activity, by cholesterol depletion using methyl-β-cyclodextrin (MβCD), which extracts cholesterol from membranes.[39] A short-term (60-minute) treatment with 1% MβCD did not change the gross morphology of cultured cells at these concentrations (data not shown) and decreased nonesterified cholesterol to 7.7% of controls. When R28 cells subsequently are treated with insulin after cholesterol depletion, activation of p70 S6K was reduced drastically by 79.2% ($P < 0.01$) in the presence of MβCD (Fig. 5A). In contrast, cholesterol depletion did not reduce and, in fact, induced ERK1/2 phosphorylation.

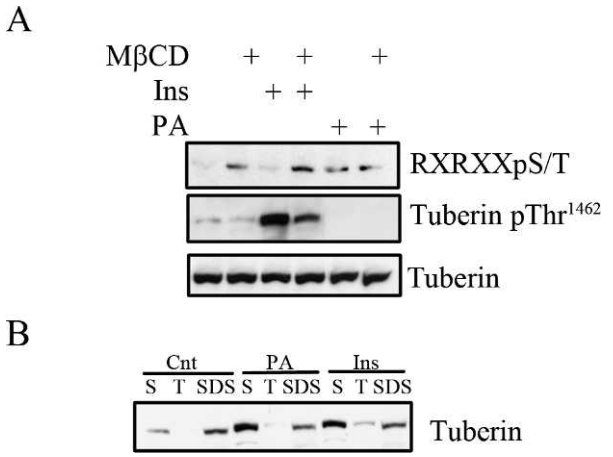

Figure 6. Insulin and PA phosphorylate tuberin and cause tuberin translocation from lipid membrane microdomains. (**A**) R28 cells in some cases were pretreated with MβCD (1%, 1 hour) before being treated with insulin or PA for 15 minutes before lysis and immunoprecipitated with an anti-tuberin antibody. The phosphorylation state of tuberin was assessed with an RXRXXpS/T motif antibody or a phospho-specific anti-tuberin Thr^{1462} antibody before assessing total levels of tuberin. ($n = 3$ for MβCD treated cells, $n = 6$ for the remaining conditions). (**B**) Treated R28 cells were fractionated as described in Figure 4A to obtain the cytosolic/soluble (S), Triton X-100 soluble (T), and SDS solublized (SDS) fractions. The fractions were analyzed by Western blotting for tuberin. Blots are representative of four independent experiments. (Fractionation controls are shown in Fig. 4A).

The effects of cholesterol depletion on PA-induced signaling also were examined (Fig. 5B). Here, similar to the effects of insulin, cholesterol depletion limited p70 S6K activation by PA. In contrast, PA stimulated ERK1/2, even in the presence of MβCD, whereas insulin does not. As an alternative to MβCD-dependent cholesterol depletion, we also used nystatin to sequester membrane cholesterol. Use of nystatin produced similar results compared to MβCD use (Fig. 5C). Like MβCD, nystatin reduced insulin (82.4%, $P < 0.01$) and PA (89.5%, $P < 0.01$)-stimulated p70 S6K, and the phosphorylation of ERK was stimulated by the presence of nystatin. Therefore, activation of the mTOR effector p70 S6K, but not ERK, by insulin and PA is cholesterol-sensitive and further suggests that PA-enriched microdomains regulate insulin-activated mTOR pro-survival signaling.

To confirm further the cholesterol-sensitivity of PA- and insulin-activated S6 kinase activity, we next performed cholesterol-repletion assays to determine if this could restore p70 S6K signaling (Fig. 5D). Similar to Figures 5A and 5B, cholesterol depletion impaired p70 S6K phosphorylation by 84.6% ($P < 0.01$) and 92.4% ($P < 0.01$) for insulin and PA, respectively. However, when cholesterol was added back after depletion, PA and insulin again were able to restore partially p70 S6K to 55.8% ($P < 0.05$) for insulin and 51.5% ($P < 0.01$) for PA compared to the agonists alone (Fig. 5D).

We also assessed the effect of cholesterol depletion on mTOR itself, Specifically, we performed a kinase activity assay on immunoprecipitated mTOR, determining the ability of the immunoprecipitated protein to phosphorylate recombinant 4EBP1. Here, we observed that insulin and PA treatment significantly augmented the activity of mTOR, which subsequently was inhibited by cholesterol depletion, resulting in a reduction by 73.6% for insulin ($P < 0.05$) and 62.8% ($P < 0.01$) for PA (Fig. 5E). Taken together, these multiple experiments demonstrated that regulation of mTOR/S6kinase activity is mediated within functional lipid microdomains.

Insulin and PA Lead to Differential Phosphorlyation of Tuberin and Diminishes Tuberin Content within Rafts

To explore further the biochemical consequences of the biophysical mechanisms by which lipid (PA) and non-lipid (insulin) agonists activate mTOR signaling through co-localization within lipid rafts, we analyzed the phosphorylation state of tuberin (Fig. 6A). Tuberin and hamartin form the tuberous sclerosis complex, which negatively regulates mTOR signaling. This negative regulation can be abrogated through phosphorylation of tuberin by upstream kinases.[40] After treatment of R28 cells with insulin or PA, tuberin was immunoprecipitated and the phosphorylation state was assessed by immunoblotting with two different antibodies, the first of which is a phosphothreonine-specific antibody to tuberin at position 1462. We observed a marked increase in threonine 1462 phosphorylation in cells stimulated with insulin, but not PA, which was inhibited by pretreatment with MβCD. The second antibody, an RXRXXpS/T phospho-motif antibody, was used as Ser^{1798}, which lies within this RXRXXS/T motif, is a major phosphorylation target of phorbol ester stimulation of tuberin.[40] In contrast to the $pThr^{1462}$ antibody, increased immunoreactivity toward the $pSer^{1798}$ motif was observed in PA-treated, but not vehicle- or insulin-treated cells. In MβCD treated cells, we observed increased basal phosphorylation at this site, which was not augmented with PA. Furthermore, phosphorylation of tuberin within the RXRXXpS/T phospho-motif in MβCD-treated cells, suggests that the cholesterol-dependent regulation of p70 S6K phosphorylation occurs downstream of tuberin at this site(s). As these sites have been shown previously to release the inhibition of tuberin on mTOR signaling,[41,42] differential phosphorylation of tuberin by PA and insulin could explain the cooperativity observed with PA and insulin upon mTOR/p70 S6Kinase/prosurvival signaling.

To assess further the cooperative effect of insulin and PA on tuberin, we also determined the localization within the cytosolic (S), Triton X-100 soluble (T), and Triton X-100 insoluble fractions (SDS, Fig. 6B). Under basal conditions, tuberin is localized predominantly to the (S) and (SDS) fractions (33.3 ± 3.3% SE and 66.1% ± 3.6% SE respectively), with highest expression in the (SDS) fraction. Upon stimulation with either insulin or PA, an increased percentage is observed in the (S) fraction (62.7 ± 3.7% SE, $P < 0.01$ for PA and 55.3 ± 4.8% SE, $P < 0.01$ for Ins) with diminished amount in the (SDS) fraction (33.3 ± 2.9%, $P < 0.01$ for PA and 38.3 ± 4.2%, $P < 0.01$ SE for Ins). This result suggested that the consequence of differential phosphorylation of tuberin by PA and insulin within microdomains is reduced tuberin content within these lipid microdomains. Thus, the convergence of these lipid and non-lipid pathways to augment mTOR-dependent survival actually may reflect the reduction of phosphorylated tuberin within lipid rafts, releasing the inhibition on mTOR signaling.

Discussion

Neuronal apoptosis in diabetic retinopathy is an early pathologic feature that precedes vascular occlusion. This neuronal cell death has been characterized in humans afflicted with diabetes and in animal models, and may underlie vision loss.[1–4] Cellular death can arise as a consequence of dysregulated signaling cascades. We characterized previously that the rat and mouse retinas are an insulin-responsive tissue that demonstrates reduced pro-survival insulin receptor, PI_3K-

Akt, and p70 S6K signaling when diabetes is induced.[12,43,44] Therefore, further understanding of the biophysical and biochemical regulation of these pathways may provide insights into therapeutic interventions to restore or augment diminished insulin signaling. Regardless of the underlying mechanism of diabetic retinopathy (hyperglycemia, inflammation, reactive oxygen species, and so forth), the critical new finding in our work is that repletion of PA mass with insulin treatment reduces retinal neuronal death. The novelty of our work lies in the potential of modifying glycerolipid metabolism to restore mTOR pro-survival signaling in diabetic retinopathy. This potential arises out of our finding that PA, a phospholipid, is diminished significantly in hyperglycemic retinal neuronal cultures and in retinas of STZ-induced diabetic rats (Fig. 1). Alluding to therapy, in an in vitro model of retinal neurons, exogenous application of PA and/or insulin-reduced IL-1β-induced cell death partly through a partially rapamycin-sensitive/mTOR mechanism (Fig. 2).

The ability of lipid microdomains to mediate insulin prosurvival signaling emphasizes the importance of the lipid environment, in general, to support homeostatic signaling. To substantiate this postulate, we demonstrate that PA and mTOR signaling elements colocalize to cholesterol-resistant microdomains (Fig. 4) with tuberin moving out of these domains upon insulin stimulation (Fig. 6). Moreover, raft dissolution via cholesterol-depletion or cholesterol sequestration disrupts insulin and PA-induced mTOR signaling (Fig. 5). This is not the first report of altered lipid content, or dysfunctional lipid signaling or topography in diabetic retinas. Increasing evidence points to altered lipid metabolism within the diabetic retina. In addition to the present study demonstrating that PA levels are diminished in hyperglycemic and diabetic models, we reported previously that within the sphingolipid class of lipids, ceramides are decreased with a concomitant increase in glucosylceramides,[30] and others have demonstrated significant decreases in retinal polyunsaturated fatty acids.[31] Thus, further understanding of changes in individual lipid components and lipid subcellular topography is of importance for understanding diabetic retinopathy. Documentation of decreased PA content within individual cell types or retinal layers presently is not feasible by mass spectrometry-based imaging due to poor sensitivity. Our data suggest that pharmacologically restoring PA concentrations within lipid microdomains could benefit retina neurodegenerative diseases by restoring the critical balance of pro-survival and pro-apoptotic signaling cascades.

We have shown that exogenous PA administration can protect against cytokine stress-induced retinal cell death, and it can be envisioned that activation of DAG kinase or PLD activities, or reduction in PA phosphohydrolase activity also can augment diminished PA levels in diabetic models. In fact, augmenting PA concentration at the expense of diglycerides, which decrease insulin signaling though the activation of protein kinase C isoforms,[45] may improve synergistically diabetic complication outcomes. Evidence supporting a role for increased DAG and/or diminished PA in diabetic complications include studies demonstrating that inhibition of diacylglycerol kinase, an enzyme that produces PA through the phosphorylation of diglycerides, mimics diabetes-induced abnormal retinal hemodynamics.[32] Furthermore, d-alpha-tocopherol (vitamin E) can limit hyperglycemic-induced diglyceride-PKC activation by enhancing DAG kinase activity.[46] Additional evidence supporting a putative regulatory role for PA is observed in RNA interference studies that have demonstrated that knockdown of the DAG kinase α or β isoforms increase apoptosis.[47] In addition, production of DAG either directly via phospholipase C[36] or as a consequence of hyperglycemia through de novo synthesis of PA and subsequent dephosphorylation of PA, has been argued.[48] Thus, shunting DAG metabolism to form PA may be desirable therapeutically to prevent diabetic complications. In fact, PA metabolism may generate other pro-survival lipid species, such as lysophosphatidic acid, which signal via EDG receptors.

PA has been shown to be a positive mediator of mTORC1 signaling through direct binding to the FKBP12-rapamycin-binding (FRB) domain of mTOR.[22] Alternatively, PA also may bind to and positively regulate Raf-1,[49] an upstream signaling molecule of the MEK cascade, which can lead to phosphorylation and inactivation of tuberin.[50,51] Yet, our results argue for an additional biophysical component by which PA-enriched membrane microdomains augment insulin-dependent mTOR/p70 S6Kinase prosurvival cascades. Similar to our results, the Romero laboratory also recently demonstrated that PA forms PA-enriched membrane microdomains.[52] This is important as microdomains can serve as sites of endocytosis, which is important for mTOR signaling[53] and presumably could offer a physiologic correlate for diminished tuberin content within microdomains.

Interestingly, while insulin does not generate PA, and PA and insulin both lead to mTOR/p70 S6K activation through different mechanisms, the pathways appear to converge at the level of the TSC complex of tuberin and hamartin. The TSC complex impairs mTOR signaling and phosphorylation of tuberin relieves this inhibition.[41,42,51] We demonstrated that these agonists differentially phosphorylate tuberin, with insulin increasing the phosphorylation of Thr^{1462}, whereas PA had no appreciable effect at this site. In contrast, PA leads to increased phosphorylation detected by a motif-specific antibody, presumably Ser^{1798} as identified by the Blenis laboratory,[42] though insulin did not have the same effect. Thus, the cooperative effect observed in lipid (PA) and non-lipid (insulin) inhibition of IL-1β-induced cellular death may be mediated through this differential phosphorylation of tuberin to augment downstream mTOR signaling components localized within functional lipid microdomains. The observation that tuberin content was diminished within these PA-enriched domains provides another explanation for the cooperative actions of insulin and PA to augment mTOR/p70 S6 kinase prosurvival signaling. It should be noted, however, that rapamycin did not block insulin and/or PA-mediated cell survival effects completely. Thus, rapamycin-insensitive (mTORC1-independent) pathways are activated that also promote retinal cell survival, which may include a phosphatidylinositol 3-kinase/Akt-mediated mechanism as described previously.[26] Interestingly, rapamycin can confer neuroprotection in other models through induction of autophagy and in the presence of overactivated mTOR.[54] As diminished p70 S6K is seen in the diabetic retina[12] and we do not observe an effect by rapamycin by itself on survival (Fig. 2A and the study of Wu et al.[11]), this neuroprotective mechanism appears to be unlikely in this model. However, this may reflect the critical balance of mTOR signaling, where elevated or diminished signaling may contribute to pathology.

In conclusion, PA-enriched, mTOR-localized, membrane microdomains may have the capability to compensate cooperatively for the diminished insulin sensitivity observed in diabetes. Enhancing insulin-dependent mTOR signaling by shunting DAG metabolism to PA or by increasing PA through exogenous application may prevent neuronal apoptosis in diabetic retinopathy and other neurodegenerations.

References

1. Bloodworth JM Jr. Diabetic retinopathy. *Diabetes*. 1962;11:1–22.
2. Barber AJ, Lieth E, Khin SA, Antonetti DA, Buchanan AG, Gardner TW. Neural apoptosis in the retina during experi-

mental and human diabetes. Early onset and effect of insulin. *J Clin Invest*. 1998;102:783–791.

3. Hammes HP, Federoff HJ, Brownlee M. Nerve growth factor prevents both neuroretinal programmed cell death and capillary pathology in experimental diabetes. *Mol Med*. 1995;1:527–534.
4. Wolter JR. Diabetic retinopathy. *Am J Ophthalmol*. 1961;51: 1123–1141.
5. Tee AR, Blenis J. mTOR, translational control and human disease. *Semin Cell Dev Biol*. 2005;16:29–37.
6. Sarbassov dos D, Ali SM, Sabatini DM. Growing roles for the mTOR pathway. *Curr Opin Cell Biol*. 2005;17:596–603.
7. Harada H, Andersen JS, Mann M, Terada N, Korsmeyer SJ. p70S6 kinase signals cell survival as well as growth, inactivating the pro-apoptotic molecule BAD. *Proc Natl Acad Sci U S A*. 2001;98:9666–9670.
8. Hui L, Rodrik V, Pielak RM, Knirr S, Zheng Y, Foster DA. mTOR-dependent suppression of protein phosphatase 2A is critical for phospholipase D survival signals in human breast cancer cells. *J Biol Chem*. 2005;280:35829–35835.
9. Huang S, Shu L, Easton J, et al. Inhibition of mammalian target of rapamycin activates apoptosis signal-regulating kinase 1 signaling by suppressing protein phosphatase 5 activity. *J Biol Chem*. 2004;279:36490–36496.
10. Meijer AJ, Codogno P. Regulation and role of autophagy in mammalian cells. *Int J Biochem Cell Biol*. 2004;36:2445–2462.
11. Wu X, Reite, CE, Antonetti DA, Kimball SR, Jefferson LS, Gardner TW. Insulin promotes rat retinal neuronal cell survival in a p70S6K-dependent manner. *J Biol Chem*. 2004;279:9167–9175.
12. Reiter CE, Wu X, Sandirasegarane L, et al. Diabetes reduces basal retinal insulin receptor signaling: reversal with systemic and local insulin. *Diabetes*. 2006;55:1148–1156.
13. Carmo A, Cunha-Vaz JG, Carvalho AP, Lopes MC. L-arginine transport in retinas from streptozotocin diabetic rats: correlation with the level of IL-1 beta and NO synthase activity. *Vision Res*. 1999;39:3817–3823.
14. Gerhardinger C, Costa MB, Coulombe MC, Toth I, Hoehn T, Grosu P. Expression of acute-phase response proteins in retinal Müller cells in diabetes. *Invest Ophthalmol Vis Sci*. 2005;46: 349–357.
15. Krady JK, Basu A, Allen CM, et al. Minocycline reduces proinflammatory cytokine expression, microglial activation, and caspase-3 activation in a rodent model of diabetic retinopathy. *Diabetes*. 2005;54:1559–1565.
16. Yoneda S, Tanihara H, Kido N, et al. Interleukin-1beta mediates ischemic injury in the rat retina. *Exp Eye Res*. 2001;73:661–667.
17. Lazovic J, Basu A, Lin HW, et al. Neuroinflammation and both cytotoxic and vasogenic edema are reduced in interleukin-1 type 1 receptor-deficient mice conferring neuroprotection. *Stroke*. 2005;36:2226–2231.
18. Basu A, Lazovic J, Krady JK, et al. Interleukin-1 and the interleukin-1 type 1 receptor are essential for the progressive neurodegeneration that ensues subsequent to a mild hypoxic/ischemic injury. *J Cereb Blood Flow Metab*. 2005;25:17–29.
19. Althausen S, Mengesdorf T, Mies G, et al. Changes in the phosphorylation of initiation factor eIF-2alpha, elongation factor eEF-2 and p70 S6 kinase after transient focal cerebral ischaemia in mice. *J Neurochem*. 2001;78:779–787.
20. Avila-Flores A, Santos T, Rincon E, Merida I. Modulation of the mammalian target of rapamycin pathway by diacylglycerol kinase-produced phosphatidic acid. *J Biol Chem*. 2005;280: 10091–10099.
21. Ballou LM, Jiang YP, Du G, Frohman MA, Lin RZ. Ca(2+)- and phospholipase D-dependent and -independent pathways activate mTOR signaling. *FEBS Lett*. 2003;550:51–56.
22. Fang Y, Vilella-Bach M, Bachmann R, Flanigan A, Chen J. Phosphatidic acid-mediated mitogenic activation of mTOR signaling. *Science*. 2001;294:1942–1945.
23. Golub T, Wacha S, Caroni P. Spatial and temporal control of signaling through lipid rafts. *Curr Opin Neurobiol*. 2004;14: 542–550.
24. Kester M, Kolesnick R. Sphingolipids as therapeutics. *Pharmacol Res*. 2003;47:365–371.
25. Seigel GM. Establishment of an E1A-immortalized retinal cell culture. *In Vitro Cell Dev Biol Anim*. 1996;32:66–68.
26. Barber AJ, Nakamura M, Wolpert EB, et al. Insulin rescues retinal neurons from apoptosis by a phosphatidylinositol 3-kinase/Akt-mediated mechanism that reduces the activation of caspase-3. *J Biol Chem*. 2001;276:32814–32821.
27. Cheng H, Jiang X, Han X. Alterations in lipid homeostasis of mouse dorsal root ganglia induced by apolipoprotein E deficiency: a shotgun lipidomics study. *J Neurochem*. 2007; 101:57–76.
28. Song KS, Li S, Okamoto T, Quilliam LA, Sargiacomo M, Lisanti MP. Co-purification and direct interaction of Ras with caveolin, an integral membrane protein of caveolae microdomains. Detergent-free purification of caveolae microdomains. *J Biol Chem*. 1996;271:9690–9697.
29. Jones KA, Jiang X, Yamamoto Y, Yeung RS. Tuberin is a component of lipid rafts and mediates caveolin-1 localization: role of TSC2 in post-Golgi transport. *Exp Cell Res*. 2004;295: 512–524.
30. Fox TE, Han X, Kelly S, et al. Diabetes alters sphingolipid metabolism in the retina: a potential mechanism of cell death in diabetic retinopathy. *Diabetes*. 2006;55:3573–3580.
31. Tikhonenko M, Lydic TA, Wang Y, et al. Remodeling of retinal fatty acids in an animal model of diabetes: a decrease in long-chain polyunsaturated fatty acids is associated with a decrease in fatty acid elongases Elovl2 and Elovl4. *Diabetes*. 59:219–227.
32. Bursell SE, Takagi C, Clermont AC, et al. Specific retinal diacylglycerol and protein kinase C beta isoform modulation mimics abnormal retinal hemodynamics in diabetic rats. *Invest Ophthalmol Vis Sci*. 1997;38:2711–2720.
33. Nakamura M, Barber AJ, Antonetti DA, et al. Excessive hexosamines block the neuroprotective effect of insulin and induce apoptosis in retinal neurons. *J Biol Chem*. 2001;276: 43748–43755.
34. Santiago AR, Cristovao AJ, Santos PF, Carvalho CM, Ambrosio AF. High glucose induces caspase-independent cell death in retinal neural cells. *Neurobiol Dis*. 2007;25:464–472.
35. Demircan N, Safran BG, Soylu M, Ozcan AA, Sizmaz S. Determination of vitreous interleukin-1 (IL-1) and tumour necrosis factor (TNF) levels in proliferative diabetic retinopathy. *Eye*. 2006;20:1366–1369.
36. Abcouwer SF, Shanmugam S, Gomez PF, et al. Effect of IL-1beta on survival and energy metabolism of R28 and RGC-5 retinal neurons. *Invest Ophthalmol Vis Sci*. 2008;49:5581–5592.
37. Lehman N, Ledford B, Di Fulvio M, Frondorf K, McPhail LC, Gomez-Cambronero J. Phospholipase D2-derived phosphatidic acid binds to and activates ribosomal p70 S6 kinase independently of mTOR. *Faseb J*. 2007;21:1075–1087.
38. Mendez AJ, Lin G, Wade DP, Lawn RM, Oram JF. Membrane lipid domains distinct from cholesterol/sphingomyelin-rich rafts are involved in the ABCA1-mediated lipid secretory pathway. *J Biol Chem*. 2001;276:3158–3166.
39. Christian AE, Haynes MP, Phillips MC, Rothblat GH. Use of cyclodextrins for manipulating cellular cholesterol content. *J Lipid Res*. 1997;38:2264–2272.

40. Jozwiak J, Jozwiak S, Grzela T, Lazarczyk M. Positive and negative regulation of TSC2 activity and its effects on downstream effectors of the mTOR pathway. *Neuromolecular Med*. 2005;7:287–296.
41. Tee AR, Fingar DC, Manning BD, Kwiatkowski DJ, Cantley LC, Blenis J. Tuberous sclerosis complex-1 and -2 gene products function together to inhibit mammalian target of rapamycin (mTOR)-mediated downstream signaling. *Proc Natl Acad Sci U S A*. 2002;99:13571–13576.
42. Roux PP, Ballif BA, Anjum R, Gygi SP, Blenis J. Tumor-promoting phorbol esters and activated Ras inactivate the tuberous sclerosis tumor suppressor complex via p90 ribosomal S6 kinase. *Proc Natl Acad Sci U S A*. 2004;101: 13489–13494.
43. Reiter CE, Sandirasegarane L, Wolpert EB, et al. Characterization of insulin signaling in rat retina in vivo and ex vivo. *Am J Physiol Endocrinol Metab*. 2003;285:E763–E774.
44. Barber AJ, Antonetti DA, Kern TS, et al. The Ins2Akita mouse as a model of early retinal complications in diabetes. *Invest Ophthalmol Vis Sci*. 2005;46:2210–2218.
45. Watson ML, Coghlan M, Hundal HS. Modulating serine palmitoyl transferase (SPT) expression and activity unveils a crucial role in lipid-induced insulin resistance in rat skeletal muscle cells. *Biochem J*. 2008;417:791–801.
46. Lee IK, Koya D, Ishi H, Kanoh H, King GL. d-Alpha-tocopherol prevents the hyperglycemia induced activation of diacylglycerol (DAG)-protein kinase C (PKC) pathway in vascular smooth muscle cell by an increase of DAG kinase activity. *Diabetes Res Clin Pract*. 1999;45:183–190.
47. MacKeigan JP, Murphy LO, Blenis J. Sensitized RNAi screen of human kinases and phosphatases identifies new regulators of apoptosis and chemoresistance. *Nat Cell Biol*. 2005;7:591–600.
48. Xia P, Inoguchi T, Kern TS, Engerman RL, Oates PJ, King GL. Characterization of the mechanism for the chronic activation of diacylglycerol-protein kinase C pathway in diabetes and hypergalactosemia. *Diabetes*. 1994;43:1122–1129.
49. Rizzo MA, Shome K, Watkins SC, Romero G. The recruitment of Raf-1 to membranes is mediated by direct interaction with phosphatidic acid and is independent of association with Ras. *J Biol Chem*. 2000;275:23911–23918.
50. Rolfe M, McLeod LE, Pratt PF, Proud CG. Activation of protein synthesis in cardiomyocytes by the hypertrophic agent phenylephrine requires the activation of ERK and involves phosphorylation of tuberous sclerosis complex 2 (TSC2). *Biochem J*. 2005;388:973–984.
51. Tee AR, Anjum R, Blenis J. Inactivation of the tuberous sclerosis complex-1 and -2 gene products occurs by phosphoinositide 3-kinase/Akt-dependent and -independent phosphorylation of tuberin. *J Biol Chem*. 2003;278:37288–37296.
52. Kraft CA, Garrido JL, Fluharty E, Leiva-Vega L, Romero G. Role of phosphatidic acid in the coupling of the ERK cascade. *J Biol Chem*. 2008;283:36636–36645.
53. Flinn RJ, Yan Y, Goswami S, Parker PJ, Backer JM. The late endosome is essential for mTORC1 signaling. *Mol Biol Cell*. 21:833–841.
54. Bove J, Martinez-Vicente M, Vila M. Fighting neurodegeneration with rapamycin: mechanistic insights. *Nat Rev Neurosci*. 12:437–452.